

**INTERANNUAL VARIATIONS IN THE ZONAL ASYMMETRY OF THE SUBPOLAR  
LATITUDES TOTAL OZONE COLUMN DURING THE AUSTRAL SPRING**

*Eduardo A. Agosta<sup>1,2</sup> and Pablo O. Canziani<sup>1,2</sup>*

<sup>1</sup> Equipo Interdisciplinario Para el Estudio de Procesos Atmosféricos en el Cambio Global – PEPACG. Pontificia Universidad Católica Argentina Santa María de los Buenos Aires, Buenos Aires, Argentina [eduardo\\_agosta@uca.edu.ar](mailto:eduardo_agosta@uca.edu.ar)

<sup>2</sup> Consejo Nacional de Investigaciones Científicas y Tecnológicas – CONICET, Argentina [canziani@uca.edu.ar](mailto:canziani@uca.edu.ar)

**ABSTRACT**

The Southern Hemisphere midlatitude Total Ozone Column (TOC) shows a “horseshoe” like structure with a minimum which appears to have two preferential extreme positions during October: one, near southern South America, the other, near the Greenwich Meridian approximately. The interannual zonal ozone asymmetry exists independently of the variations induced by the 11-year solar cycle, the Quasi-Biennial Oscillation (QBO) and planetary wave activity inducing the Brewer-Dobson circulation. The classification and climatological composition of these two extreme ozone-minimum positions allows for the observations of statistically significant patterns in geopotential height and zonal winds associated with the quasi-stationary wave 1, extending throughout lower stratosphere. The changes in the quasi-stationary wave 1 associated with the extreme TOC positions appear to have sinks and sources determining transient interactions between troposphere and the stratosphere. Thus, distinct climate states in the troposphere seem to be dynamically linked with the state of the stratosphere and ozone layer. The migration of the TOC trough from southern South America to the east during the 1990s can be related to changes in the troposphere/stratosphere coupling through changes in the Southern Annular Mode variability in spring.

**Keywords:** Total Ozone Column, stratosphere/troposphere coupling, climate variability

**RESUMEN**

La Columna Total de Ozono (CTO) de las latitudes medias del Hemisferio Sur muestra una estructura de “herradura” con un mínimo que muestra tener dos posiciones preferenciales extremas durante octubre: uno, en las cercanías del sur de Sudamérica, y el otro, cerca del meridiano de Greenwich. La asimetría zonal de ozono existe independientemente de las variaciones inducidas por el ciclo solar de 11 años, la Oscilación Cuasi-Bianual (QBO) y la actividad de onda planetaria asociada a la circulación de Brewer-Dobson. La clasificación y composición climatológica de estas dos situaciones longitudinalmente extremas de mínimo de ozono permite observar patrones estadísticamente significativos en geopotencial y vientos zonales asociados a una onda cuasi-estacionaria 1 que abarca la estratósfera inferior. Los cambios en la onda cuasi-estacionaria 1 asociados a las posiciones extremas de mínimo de ozono muestran tener fuentes y sumideros que determinan interacciones transientes entre la troposfera y la estratosfera. Así, estados climáticos distinguibles de la troposfera parecen estar dinámicamente vinculados con el estado de la estratosfera y la capa de ozono. La migración de la vaguada de CTO desde el sur de Sudamérica hacia el este durante la década de 1990 puede estar vinculada a cambios en la variabilidad del Modo Anular del Sur durante la primavera austral.

**Palabras claves:** Columna Total de Ozono, acoplamiento estratosfera-troposfera, variabilidad climática.

## INTRODUCTION

The mid-to-subpolar latitudes spatial ozone distribution in the Southern Hemisphere (SH) presents a zonal asymmetry like a “horseshoe” from June to December, with maximum values in the Indian Ocean, south of Australia (90°E-180°E), and minimum values in the South Atlantic and southern South America (60°W-0°E). At higher latitudes over the Antarctica, the stratospheric polar vortex provides the dynamical framework for the building-up of the ozone “hole” (relatively low ozone values), due to the late winter/early spring low temperatures of isolated air masses, favoring the activation of the chlorine-UV-photolysis-ozone catalysis process. The maximum amplitude of the ozone zonal asymmetry occurs during austral spring, especially in October (Labitzke and van Loon 1999, Grytsai *et al.* 2007). An interesting feature of this horseshoe-like ozone field is that it is not similarly located year year out; instead, it rotates, varying longitudinally, in particular the ozone minima area, which conforms a midlatitude ozone trough associated to the major axis of polar ozone “hole” ellipsoid. Hence, it resembles an ozone quasi-stationary wave 1 (QSW1). The nature of the interannual ozone content variability at a certain location is largely attributed to dynamics, especially through the interaction of tropospheric planetary waves with the stratospheric mean state (Fusco and Salby 1999; Hood and Soukharev 2003; Randel *et al.* 2002). However few studies are focused on the austral spring ozone QSW1 interannual phase variability.

According to Mistaoui *et al.* (2003) the austral spring stratospheric mean state is dominated by a geopotential QSW1 whose maximum amplitude is also observed in October. This QSW1 is responsible of the ozone distribution within the mid-to-low stratosphere due to associated vertical displacements that induce density variations in that region. They stated that the background flow induced by QSW1 shows weak winds in regions over South America and propagating waves preferentially break there. Hence non-reversible mixing of ozone-poor polar vortex air into southern midlatitudes is produced just where the potential vorticity gradient is weaker. This is the main dynamical reason for which the negative midlatitude ozone trough is located there. They also noted that QSW1 does not experience phase variation year after year, but without statistical evidence to support their conclusion. More recently, Jiang *et al.* (2008) performing a Principal Component Analysis on monthly mean total ozone column (TOC) and the 30-100hPa geopotential thickness from Jan 1979 to Dec 2005, showed that their third and fourth modes exhibit wavenumber-1 structures that are not related with stationary waves in phase, contrary to Northern Hemisphere results.

At longer scales, Huth and Canziani (2001) noted, in their PCA study of Southern Hemisphere (SH) and Northern Hemisphere 600K Potential Vorticity fields, that the evolution of the Antarctic polar vortex showed important changes during the austral spring, between 1980 and 1997. They observed that the main change in seasonal evolution observed around 1990 for the SH was not present in the northern hemisphere. They also noted an eastward migration of the ozone trough over the South Atlantic Ocean. A latitude-longitude ozone trend analysis by Malanca *et al.* (2003) found that when the SH ozone trends were estimated separately for the 1980s and 1990s the peak ozone depletion trends at mid to high southern latitudes during September and October migrated eastward over the Atlantic, from southern South America towards the Greenwich Meridian. Malanca *et al.* (2005) noted significant temporal and spatial variations in the longitudinal behaviour of trends when using a polynomial (cubic) adjustment of the total ozone monthly data from TOMS measurements for mid to high southern latitudes.

They also noted that at southern midlatitudes the interannual ozone rate of change presented, at mid to high southern latitudes, a low frequency, longitude dependant, modulation where the zero amplitude node of the longitudinal pattern slowly migrated eastward south of 45°S over the 20 year period. More recently Grytsai *et al.* (2007) described the temporal evolution of total ozone at high southern latitudes and noted a long-term eastward displacement of about 45° of the quasi-stationary minimum observed over the sector 60°W-0°E, whereas the maximum takes enough stable position in the quadrant 90°E-180°E. They ascribed the zonal anomaly of low ozone in the sector 60°W-0°E to the steady displacement and elongation of the ozone “hole” under the influence of planetary waves, though they do not discuss its year-to-year longitudinal variation. In addition, inspection of total ozone stationary planetary wave amplitude evolution included in Grytsai *et al.* (2005) appear to suggest a stabilization of the seasonal amplitude of quasi-stationary wave 1 since 1990, which means that the ozone zonal asymmetry is not growing as it was during 1980s.

Furthermore, Canziani *et al.* (2008) have recently studied the decadal variations in ozone at southern midlatitudes in winter (June) and spring (October). Their results suggest that the spatial total ozone distribution over the SH midlatitudes can be modified locally, during early winter at least, by changes induced by baroclinic transients wave drag on the mean flow in the lower stratosphere. This agrees with previous case studies by Canziani and Legnani (2003) that showed that baroclinic synoptic scale disturbances of tropospheric origin can penetrate into the lower stratosphere, even above 100hPa before becoming evanescent. Canziani *et al.* (2008) showed that the transients are still present during October even if the spatial variations in total ozone induced by the QSW1 are far stronger and hence are the dominant feature. Such results suggest that the SH tropospheric transient activity could play an important role in the lower stratosphere dynamics and ozone spatial distribution. They also noted, in agreement with Moustouli *et al.* (2003) that this stratospheric wave also controlled the state of the mid-to high latitude extratropical tropopause layer (ExTL, cf. Pan *et al.* 2004, and Bischoff *et al.* 2007)

In consequence our aim is to examine the interannual phase variability of the negative area of the ozone zonal asymmetry during October at southern mid-to-high latitudes in relation with stratospheric QSW1 and the upper troposphere/lower stratosphere maximum zonal winds (jets) that are directly related with SH stormtracks. Potential links with the midlatitude ozone trough eastward migration during the last decades are discussed thus providing some additional insights on the results introduced above.

## **METHODOLOGY**

Southern Hemisphere total ozone column (TOC)  $1^{\circ} \times 1.25^{\circ}$  monthly mean fields were obtained from the retrievals made by the TOMS satellite borne family of instruments for the period 1979-2005. This sequence of monthly mean fields has a gap between April 1993 and July 1995, due to malfunction in the TOMS METEOR instrument. Meteorological information, geopotential height (HGT), temperature, U and V wind components were obtained from the NCEP reanalysis monthly mean  $2.5^{\circ} \times 2.5^{\circ}$  products for the same period.

In order to measure the October subpolar maximum TOC variability induced by dynamic processes, the solar cycle, QBO, equivalent chlorine loading (EESC) and Brewer-Dobson circulation (proxied by the vertical zonal mean EP-flux through 100hPa) contributions were estimated using a multi-regression approach considering seasonality (Ziemke *et al.*, 1997) and filtered out. In the residual field the area with maximum variance in October was determined and the local mean residual TOC was used to build a time series index for the maximum TOC variability (Max Var index), as shown in Figure. 1. Extreme values for the Max Var index series are determined using the upper and lower quartiles, and composite mean fields are obtained for the time anomalies and the zonal asymmetries at UT/LS levels.

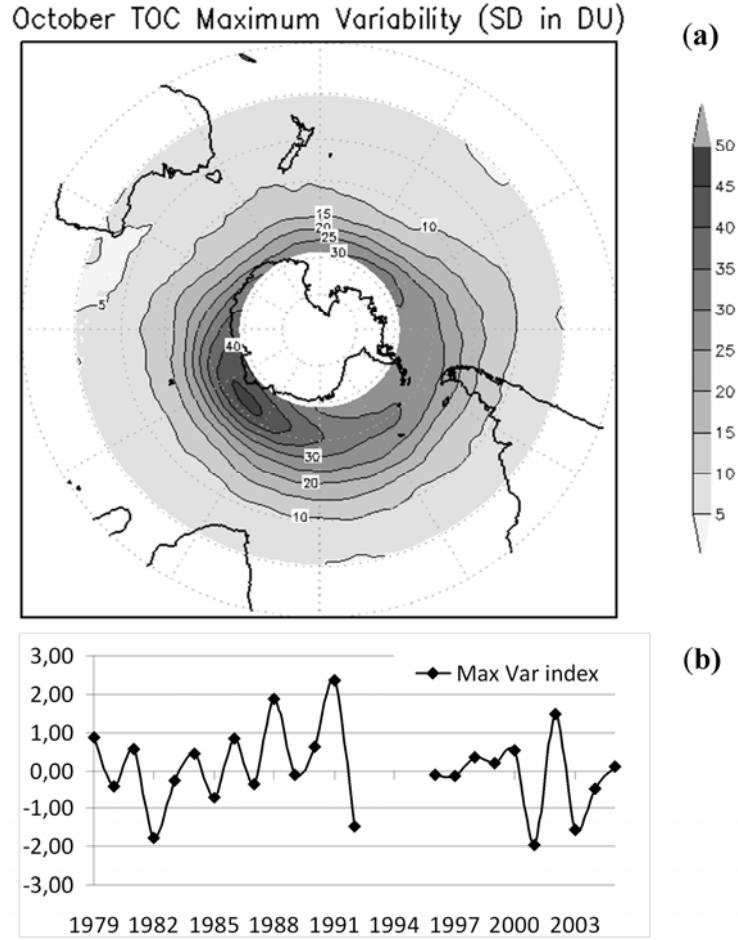


**Figure 1.** a) Residual Total Ozone Column (TOC, interval 5 DU) standard deviation map for October and b) associated adimensional time series Max Var for the area with maximum standard deviation is observed (at 61°S and 45°E).

Anomalies were tested with unequal variance two-tail t-test for sampled means (Moser *et al.*, 1989, 1992). For small amplitude waves on a zonal mean flow, the conservative relationship for stationary wave activity (Plumb, 1985) may be written as stationary wave activity for which the three-dimensional flux  $F_s$  for stationary wave is given by:

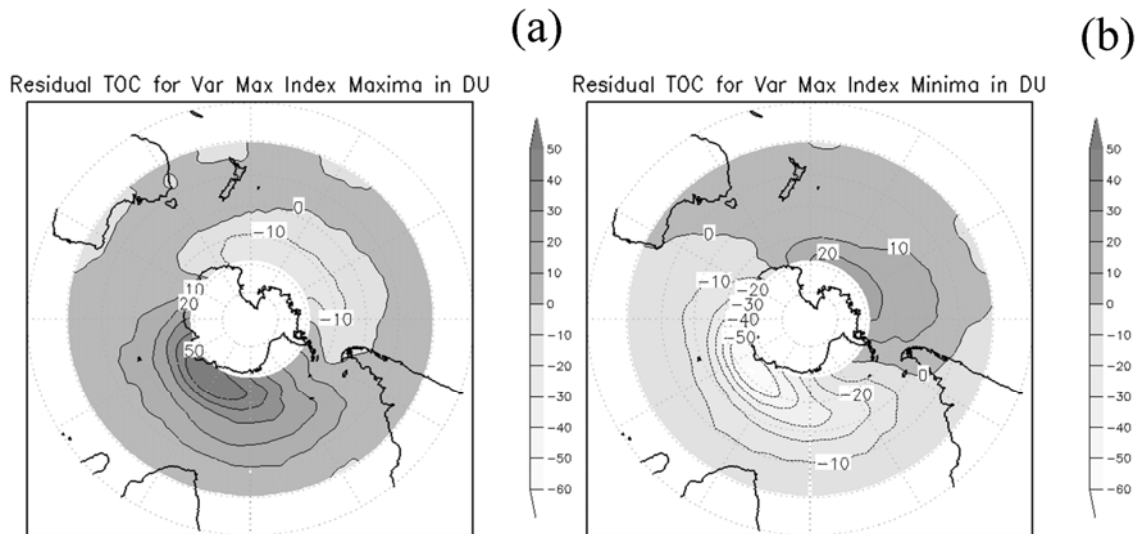
$$\begin{aligned}
 F_s = p \cos\varphi \left\{ \bar{v}^{*2} - \frac{1}{2\Omega a \sin 2\varphi} \frac{\partial(\bar{v}^* \bar{\phi}^*)}{\partial \lambda}, -\bar{u}^* \bar{v}^* \right. \\
 \left. - \frac{1}{2\Omega a \sin 2\varphi} \frac{\partial(\bar{u}^* \bar{\phi}^*)}{\partial \lambda}, \frac{2\Omega \sin\varphi}{S} \right. \\
 \left. \times \left[ \bar{v}^* \bar{T}^* - \frac{1}{2\Omega a \sin 2\varphi} \frac{\partial(\bar{T}^* \bar{\phi}^*)}{\partial \lambda} \right] \right\}
 \end{aligned}$$

Here the overbar represents a time average and the quantities with asterisks denote departures from the zonal average;  $p$  is the pressure,  $U$  is the zonal mean flow,  $u^*$  and  $v^*$  are the eddy zonal and meridional geostrophic wind components,  $a$  is the earth's radius,  $\phi$  is the geopotential,  $T$  is the temperature,  $\Omega$  is the angular rotation rate of the earth, and  $S$  is a time- and area-averaged static stability. This is applied to the monthly mean zonal asymmetries of the basic flow.  $F_s$  divergence

(convergence) can be related with stationary wave activity sources (sinks), and the  $F_s$  vectors directions indicate the stationary wave energy propagation. This study is focused in the interest of its potentiality to roughly localize stationary waves sinks and sources.

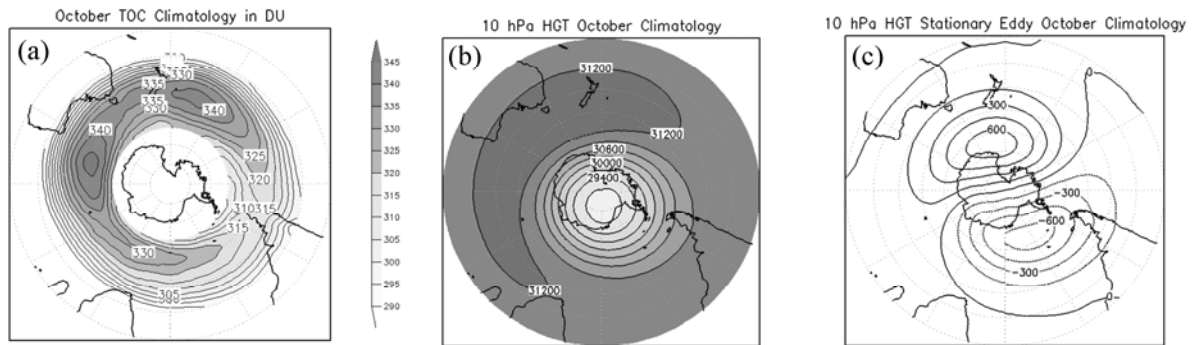
## RESULTS

Figure 2 shows the composites for October residual TOC fields identified with maximum (Fig. 2a) and minimum (Fig. 2b) index values, using the quartile index criterion. It can be seen that the index criterion captures the spatial longitudinal variation in the subpolar region that we want to analyze. During minimum index values the composited residual TOC has a dipolar structure south of 40°S with maximum values close to 30DU in the South Pacific and minimum close to -60DU at high latitudes south of Madagascar. On the other hand for maximum index composites, a weaker minimum now occurs in the South Pacific (close to -10DU) and a maximum, above 40 DU south of Madagascar. In other words there is almost a 180° phase shift in the residual anomalies between the upper and lower quartiles. These residuals, when added to the mean TOC field (Fig. 3a) describe reasonably well the zonal interannual movement observed in monthly October “horseshoe”-like TOC fields during the years sampled. Moustouli *et al.* (2003) noted that the climatic TOC minimum over the western South Atlantic and South America is further enhanced by leakage due to a preferential region for wave breaking and a reduced polar vortex gradient, which results in the non-reversible mixing of ozone-poor polar vortex air into southern midlatitudes. Bear in mind that large TOC values occur outside the polar region TOC minimum due to the meridional mass circulation established by the Brewer-Dobson circulation, resulting in the accumulation of ozone outside the polar vortex throughout the austral winter and early spring, while TOC minimum within the polar vortex occurs because it is heterogeneously destroyed within (Labitzke and van Loon 1999).



**Figure 2.** Composite residual TOC maps for maximum (a) and minimum (b) Max Var index defined using the upper ( $q_3=0.58$ ) and lower ( $q_1=-0.42$ ) quartiles Max Var index distribution. Interval is every 10 DU.

The Max Var index series in Figure 1b shows the predominance of extreme negative index values after the 1990s (66% of cases), while the extreme positive are equally distributed. The predominance of negative extreme Var Max index values is clearly attributed to the eastward migration of the mean mid-to-high latitudes ozone position trough between 80s and 90s as described by previous studies (Huth and Canziani 2001, Malanca *et al.* 2003, Malanca *et al.* 2005, Grytsai *et al.* 2007). Hence, the minima composite field features can be ascribed to low-frequency processes that drive the eastward migration.



**Figure 3.** Southern hemisphere October climatological fields for a) horseshoe-like TOC spatial mean field (interval 5 DU), b) geopotential height (HGT, interval 300 gpm), and c) stationary geopotential height eddy (interval 150 gpm). Note the strong similarity between TOC and geopotential height fields.

Figure 3b show the 10hPa HGT mean field for October. The lower stratosphere basic state is characterized by QSW1 at mid to high southern latitudes defining a stratospheric polar strong vortex extending throughout the lower and middle stratosphere, from below 100hPa. It should be noted that the mean HGT field at 10hPa closely resembles the spatial structure of the mean TOC field (Fig. 3a). Moustouli *et al.* (2003) argue the stratospheric QSW1 perturbs the isentropic surfaces, redistributing ozone in such a way that the ozone fields closely mimic the observed pattern in the stratospheric HGT field. Figure 3c shows the climatic zonal asymmetry or stationary eddy in the HGT at 10hPa, which is the spatial departure from zonal symmetry. This stationary eddy is typical from 150hPa up to mid stratosphere.

Figure 4 presents the HGT composite field composites at 10hPa for maximum (a) and minimum (b) Var Max index years, and their zonal asymmetries anomalies (c and d, respectively). Dark (light) grey shaded areas correspond to statistically significant (95%) positive (negative) asymmetry anomalies against the unequal variance t-test. Clearly there are spatial differences in HGT quasi-wave 1 structure between these two composites. During maxima the composite mean pattern is westward rotated (approx. 15-20°). The positive zonal anomaly is stronger and more elongated towards South Africa, while the negative anomaly is much weaker and found over southern South America (Fig. 4c), producing a sharper and stronger polar vortex edge over the Indian Ocean whose meridionally weak gradient, both in the polar vortex edge and midlatitude trough, faces toward southern South America (Fig. 4a).

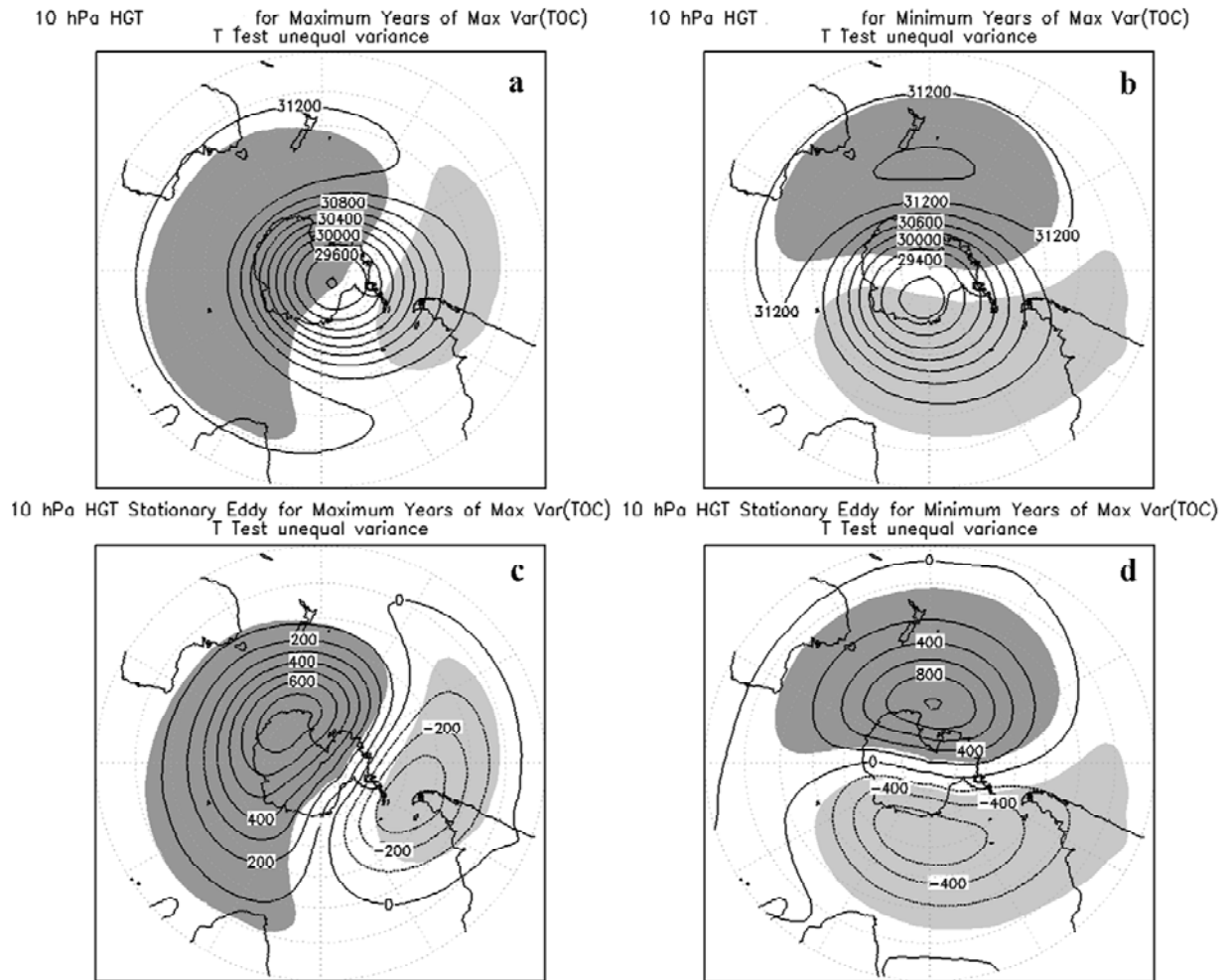


**Figure 4.** The 10hPa Geopotential height (HGT in gpm) composites (a and b) and stationary eddies (zonal asymmetry anomalies; c and d), for Max Var index maximum (left panels, a and c) and Max Var index minimum (right panels, b and d) index years. Dark (light) grey shaded areas correspond to statistically significant (95%) positive (negative) asymmetry anomalies.

During minima (Fig. 4b) there is an enhancement of the mean wave pattern, i.e., a slight strengthening of the largest HGT values in the Pacific sector and a slight weakening in the negative lobe (Fig. 4d) which mainly results in a weakening of the polar vortex gradient region (the vortex edge) as well as the midlatitude trough region over the South Atlantic and a strengthening in the South Pacific sector (Fig. 4b). In a PCA approach Hio and Hirota (2002) also found that the 10 hPa geopotential QSW1 shows two first leading modes during Sep and Oct, the first mode related with the amplitude variation and the second with the phase change with respect to the climatological mean.

A comparison of Figure 2 with Figure 4 shows that the TOC residual has its largest differences between maxima and minima in regions are coincident with gradient regions of the shifting HGT minimum in the western hemisphere. For maxima the largest positive TOC residuals coincide with the trailing edge of the positive HGT asymmetry and the negative values are collocated towards the trailing edge of the negative HGT asymmetry (Figs 2a and 4c). On the other hand during minimum index values, the negative TOC residual to the south east of South Africa is found between the trailing edge of the positive HGT asymmetry and the leading edge of the negative asymmetry and the positive TOC residuals near the trailing edge of the negative asymmetry (Figs. 2b and 4d). The overall picture for the horseshoe-like ozone pattern is that the region of TOC minima accompanies the significant polar vortex/midlatitude trough longitudinal movement (Fig. 4 a,b). This means that the prevalent meridionally weaker polar vortex edge sector, and the associated midlatitude region, are indeed acting as the dynamical containment vessel for TOC residuals and that changes in its spatial structure modify

the TOC field in agreement with Moustouai *et al* (2003). Hence the changes in TOC fields presented above must be consequence of interannual changes in the stratospheric QSW1 that modifies the polar vortex trough location.

Figure 5 shows the HGT composite field composites at 10hPa for maximum and minimum index years (left and right panels, a and b, respectively), and their temporal anomalies (lower panels, c and d). Dark (light) grey shaded areas correspond to statistically significant (95%) positive (negative) temporal anomalies against the unequal variance t-test. Between maxima and minima the anomalies show flip-flop behaviour, coincident with the observed TOC residuals (Figure. 2a-b). This further suggests that TOC residual changes are of dynamic nature. For maxima, the stronger positive temporal anomalies around Antarctica in the eastern hemisphere are predominant suggesting intense tropospheric transient planetary waves' activity in the area (Fig. 5c). The meridional HGT gradient is stronger there evidencing a strengthening of the stratospheric vortex in the polar side (Fig. 5a; see also Fig. 7b-1). For minima, the significant stronger positive anomalies in the southeastern Pacific near Antarctica reveal another active region for planetary transience (Fig. 5d). In consequence, the TOC residual zonal changes correspond to meridionally-weak polar vortex sector/trough zonal displacement that is responding to distinct active transient waves regions.

Figure 6 presents the October climatological divergence of  $F_s$  (panels 1) at 10, 50 and 100hPa (panels a, b and c) and  $F_s$  divergence for maxima (panels 2) and minima (panels 3) at the same levels, respectively. For the cases of maxima and minima only those values over a half of the maximum amplitude of the climatological field have been drawn in order to emphasize the physical significance. Recall that  $F_s$  divergence (convergence) can approximately be associated with sources (sinks) of stationary waves. The stratospheric stationary wave amplitude grows with height, for this reason the source (sinks) signatures are more precisely defined at 10hPa. This does not necessarily mean that the observed source (sink) region is confined to the level analyzed (Plumb 1985). Stationary waves are usually generated by orography and the land/sea thermal contrasts in the Northern Hemisphere (Karoly and Plumb 1989).



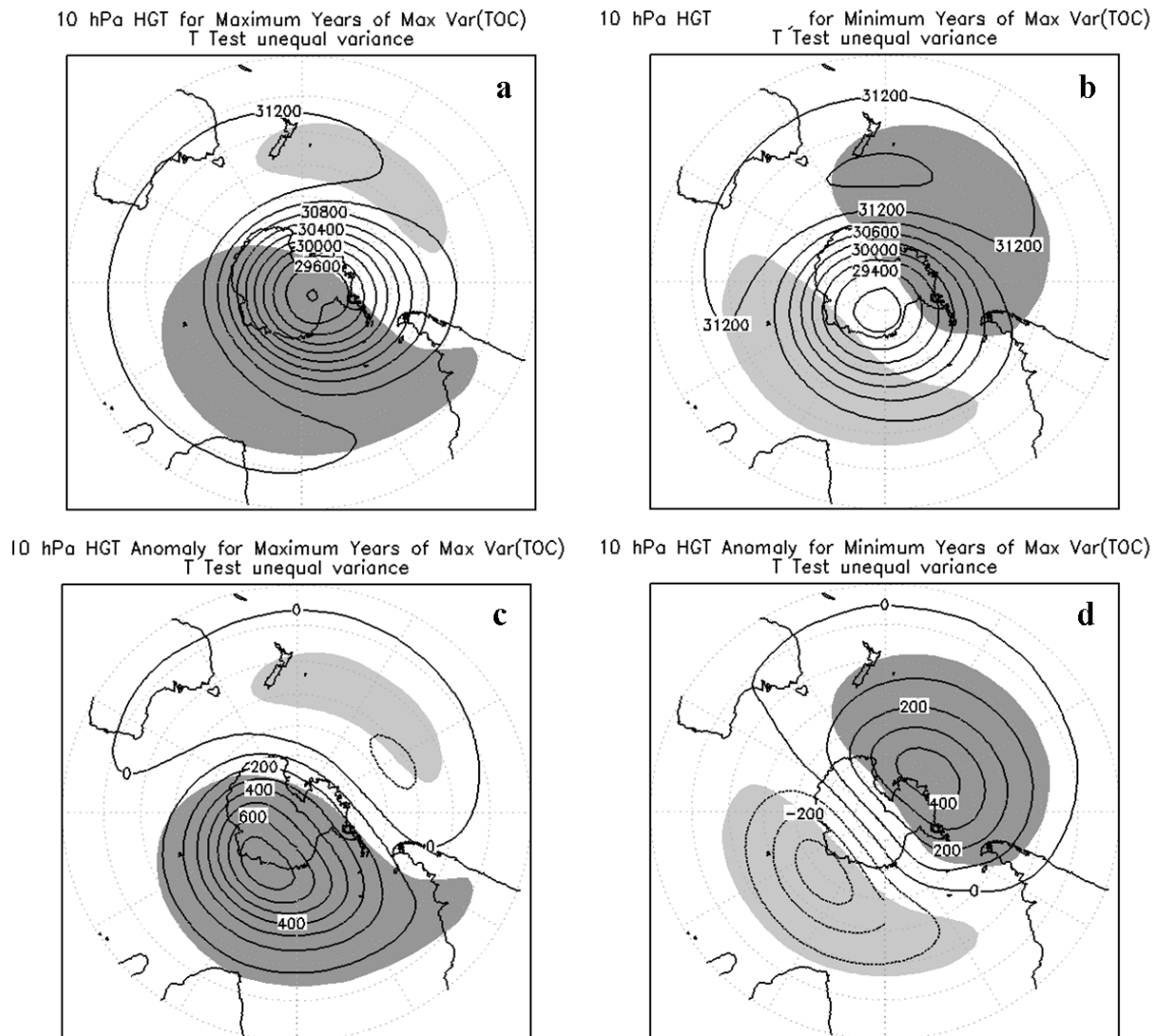


**Figure 5.** The same as upper panels in Fig. 4 but for the 10hPa HGT temporal anomalies (lower panels).

At southern high latitudes, the stationary wave sources can be related to planetary waves generated by the Antarctica orography and thermal (ice/ocean) contrasts (Rao *et al.* 2004) as well as tropospheric transient planetary waves associated to asymmetries in the upper tropospheric jets (Inatsu and Hoskins 2004). The climatological fields (Figs. 6a-1,b1 and c-1) reveal that areas over the South Pacific, South Atlantic and Indian Oceans at the mid to high latitudes as well as areas over Antarctica appear to be source regions for stratospheric quasi-stationary waves. Two preferential sites, one over the Antarctica Peninsula and the other on the opposite side of Antarctica, appear to be sink regions. The  $F_s$  divergence field at high latitudes is nearly flat below 200 hPa; instead, the stationary wave sources appear to be relevant over the mid to tropical latitudes southern continents as well as specific tropical oceanic areas (figures not shown). There, the continents' topography and the tropical latent heat release in the upper troposphere are the common source of quasi-stationary Rossby's waves (Plumb 1985). For maxima, the stratospheric  $F_s$  divergence fields show limited physical enhancements respect to the climatological fields (Figs. 6 a-2,b-2 and c-2). At 100hPa the sink region south of Tasmania near Antarctica and the source region in the South Pacific appear to be slightly enhanced (Fig. 6c-2). At 10hPa, the midlatitudes South Atlantic source region is moderately reinforced and South Pacific source region is rather wider (Fig 6a-2). For minima, the source and sink regions appear to be in quadrature highly reinforcing the observed climatological divergence fields, mainly at 10 and 50hPa (Fig. 6a-3, b-3). At 10hPa, where the stationary wave amplitude is maximum, the source regions show a slight eastward shift compared to the climatology (Fig. 6a-3 and 6a-1). In the lower

stratosphere (100hPa) the reinforcement is discernible for the source/sink regions over high latitudes in the Indian/Pacific Ocean (Fig. 6c-3), possibly suggesting a source region due to latent heat release associated to tropospheric baroclinic waves.

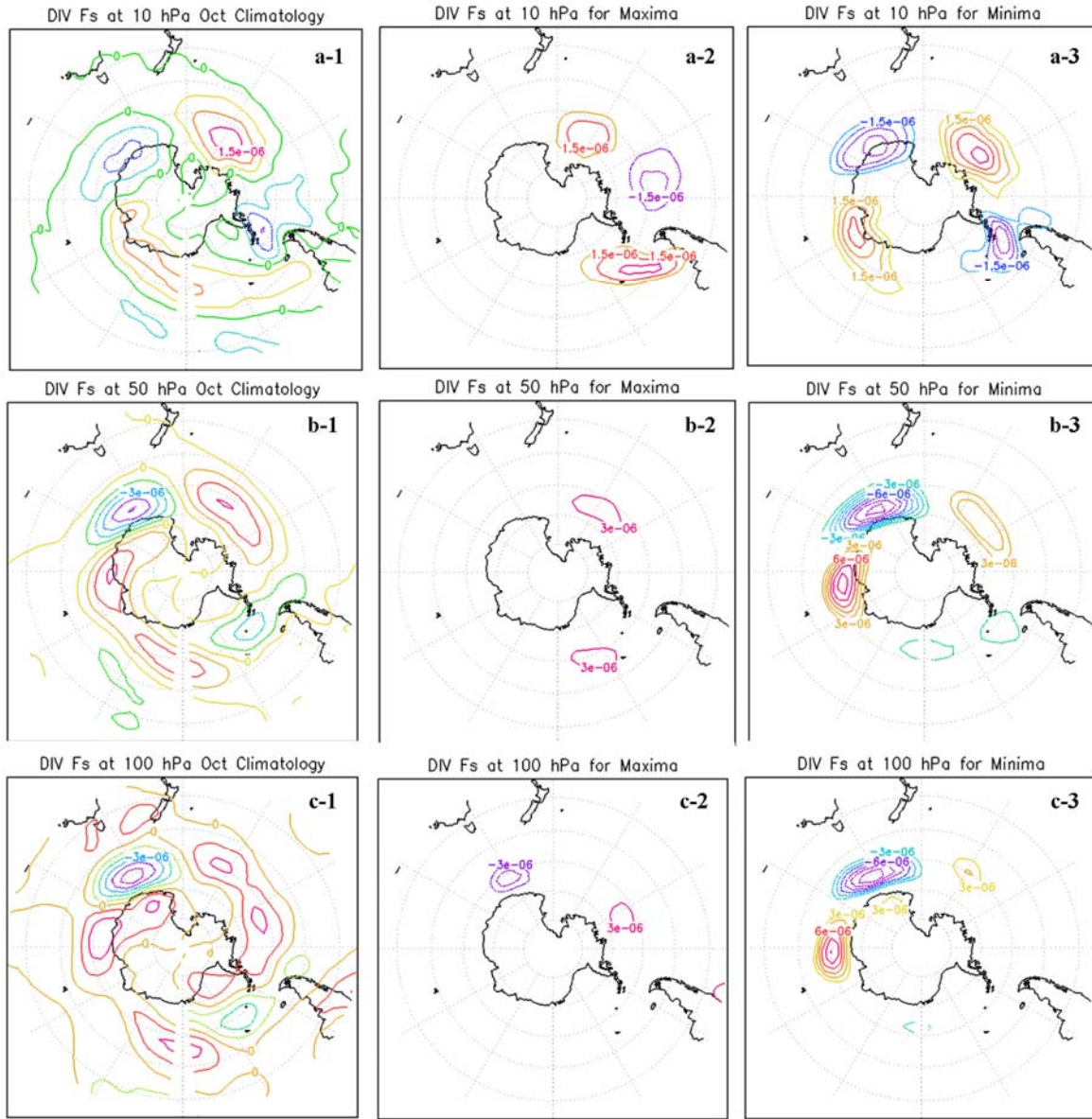


**Figure 6.** October Divergence fields of the stationary wave flux activity  $F_s$  for the climatology (panels 1), for Max Var index maxima (panels 2) and Max Var index minima (panels 3) composites at 10hPa (panel a), 50hPa (panel b) and 100hPa (panel c). Intervals are every  $10^{-6} \text{m/s}^2$  at 10 and 50hPa and every  $5 \cdot 10^{-7} \text{m/s}^2$  at 100hPa. For the composites, drawn contours are over  $7.5 \cdot 10^{-7} \text{m/s}^2$  at 10hPa,  $2.5 \cdot 10^{-6} \text{m/s}^2$  at 50hPa and  $2.0 \cdot 10^{-6} \text{m/s}^2$  at 100hPa (the half of the maximum amplitude of the corresponding climatological divergence field).

Comparison of Figure 6 with 5 shows that source (sink) regions are co-located with the extreme (transition) HGT asymmetry values in the quasi-wave 1 pattern, during minima (Fig. 6a-3 and 5d). Despite the major spatial pattern differences somewhat the same behaviour can be found for maxima (Figs. 6a-2 and 4c). As expected, this suggests that stationary wave sources act to enhance the quasi-stationary eddy while sinks, to dump their growth. Therefore, the evident change in the reinforcement of the source/sinks active regions are inducing the changes of the stationary wave number 1 observed during TOC residual maxima and minima.

Figure 7 shows the climatological zonal wind fields as well as composites for maxima and minima in the upper troposphere (300hPa) and lower stratosphere (100 and 50hPa) over the SH. Dark (light) shading implies statistically significant (at the 95% level) enhanced (weakened) zonal winds. The stratospheric polar vortex and the tropospheric polar and subtropical jets composites show significant differences between maxima and minima.

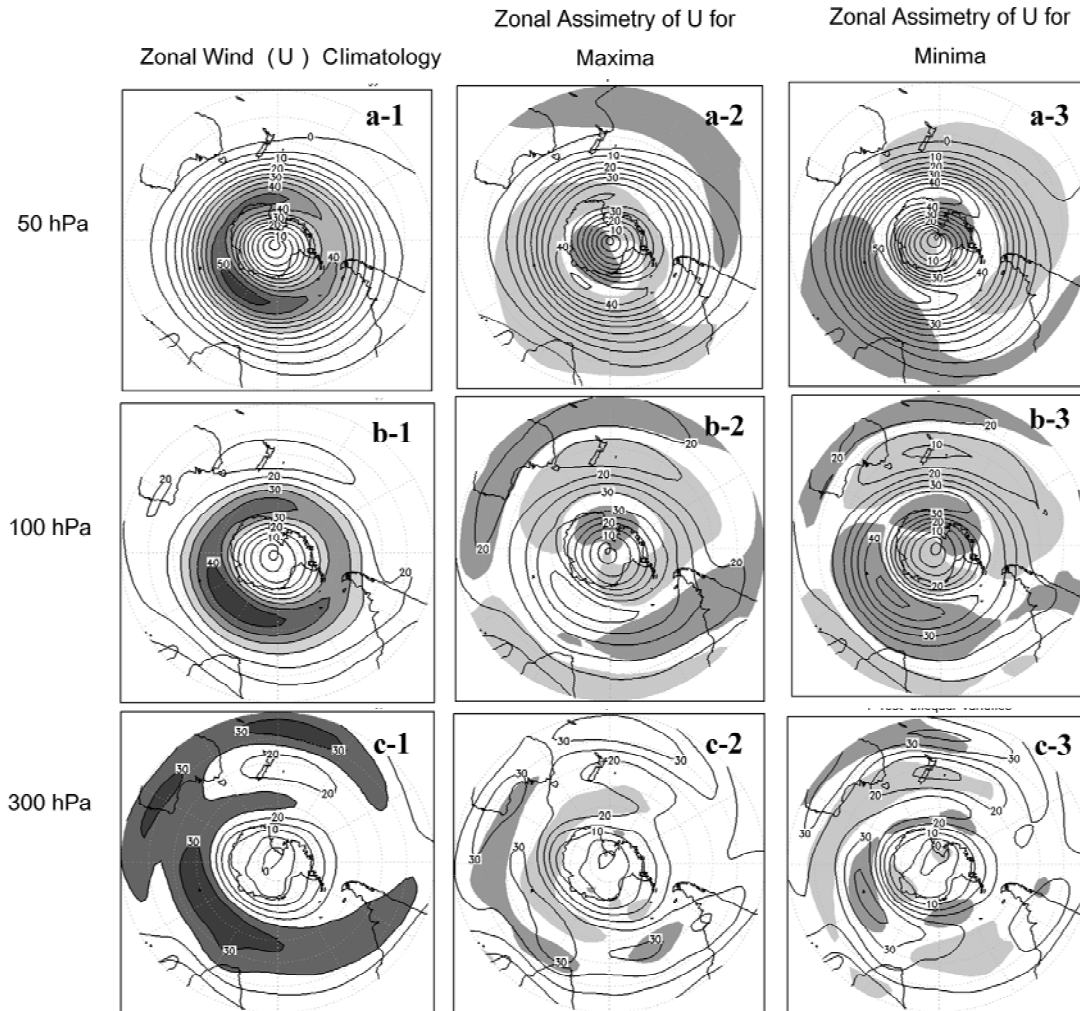


**Figure 7.** Climatological zonal wind fields (panel 1) and composites for Max Var index maxima (panel 2) and Max Var minima (panel 3) in the upper troposphere (300hPa, panel c) and lower stratosphere (100hPa, panel b, and 50hPa, panel a) over the SH: dark (light) shading implies statistically significant (at the 95% level) enhanced (weakened) zonal winds. (Units are in m/s, intervals are every 5m/s).

During maxima, at 300hPa (Fig. 7c-2) the composites show significant enhancement of the tropospheric subtropical jet over the South Atlantic, the Indian Ocean between South Africa and Southern Australia, and a significant weakening over the same longitudes in the region at the high latitudes which also extends into the South Central Pacific. The overall upper tropospheric picture is of a “single” (subtropical) jet structure over the Eastern Hemisphere. At 100hPa the subtropical enhanced wind region is more zonally extended and the high latitude weakened region is shifted further east. The upper subtropical tropospheric/lowermost stratospheric jet enhancement over the Indian and South Atlantic Oceans are partially co-located at both levels(Fig. 7c-2 and b-2), and the latter region can be associated with the stationary-wave source reinforcement there (Fig. 6b-2). The eastward extended weakened lower stratospheric wind spirals poleward reaching polar latitudes in the region

where the weaker edge of the polar vortex and trough are located during maxima, i.e., to the south of the South Cone. Note at the same time the polar region of enhanced zonal winds further south of New Zealand over Antarctica (Fig. 7b-2). At 50hPa the polar vortex enhanced/weakened wind regions correspond to the stratospheric HGT anomalies there (Fig. 7a-2 and Fig. 5c). The overall U wind enhancements and weakenings suggest a coupling between upper troposphere (300hPa) and lower stratosphere (100hPa) especially in the South Atlantic/southern South America sector. As tropospheric jets act as waveguides for baroclinic tropospheric transient waves (Trenberth 1991), zonal wind anomalies suggest an equatorward migration of the stormtracks during maxima. The stratospheric polar vortex seems to behave independently (50hPa).

During minima the zonal wind spatial changes are distinctly diverse. At 300hPa (Fig 7c-3) there are two regions of enhanced winds in the troposphere, one at mid to high latitudes from the southern South Atlantic and central Indian Oceans toward southern Western Pacific, and the other at subtropical latitudes over Australia and the Western South Pacific. At mid to subtropical latitudes there is a weakening over the South Atlantic, Indian and Western Pacific Oceans. The overall picture is that of a tropospheric “double” jet structure (Fig. 7c-3). At 100hPa similar enhanced/weakened wind areas appear zonally extended (Fig. 7b-3). At polar latitudes the wind enhancement/weakening regions agree with the stratospheric HGT anomalies (cf. Fig. 5d). At 50hPa, there is a strong wind anomaly wave 1 pattern (Fig. 7a-3), almost 180° out of phase with the maxima wind field (cf. 7a-2), affecting the stratospheric polar vortex behaviour and clearly responding to the stratospheric HGT anomaly (cf. Fig. 5d). For minima, the overall U wind enhancements and weakening suggest a coupling between the upper troposphere (300hPa) and the lower stratosphere (100hPa) over the Indian Ocean and subtropical latitudes over Australia and Western Pacific, closely located to the stationary eddy source regions (cf. Fig. 6a-3). The overall strong wind anomalies reinforce the corresponding climatology fields for each atmospheric region over the Indian Ocean sector. The stratospheric polar vortex behaves similarly from lower stratosphere to the mid stratosphere (100hPa and 50hPa).

In order to discern whether the distinct maximum zonal wind anomalies found during extreme locations of the October midlatitude ozone trough, that are associated with phase changes in the stratospheric QSW1, can be linked to synoptic scale perturbations linked to active troposphere jets, the daily probability (p) of occurrence of jet-stream is calculated for years of Var Max maxima and minima (Figures 8a and 8b, respectively). Here we define a daily jet-stream where local daily zonal winds are over 25m/s at 300hPa, and it will be simply called a jet. Our main concern is to verify whether the double jet structure observed in the monthly mean zonal winds for the minima composites can be ascribed to daily double jets occurrence, one at mid-to-subpolar latitudes and the other at subtropical-to-lower latitudes. During year of Var Max maxima (midlatitude ozone trough towards South America) the daily probability of jet occurrence is highest ( $p > 0.80$ ) along the equatorward sector of the subtropical branch of the climatological jet stream in western Pacific, extending with lower values ( $p > 0.65$ ) towards the west over Australia and the subtropical Indian Ocean.

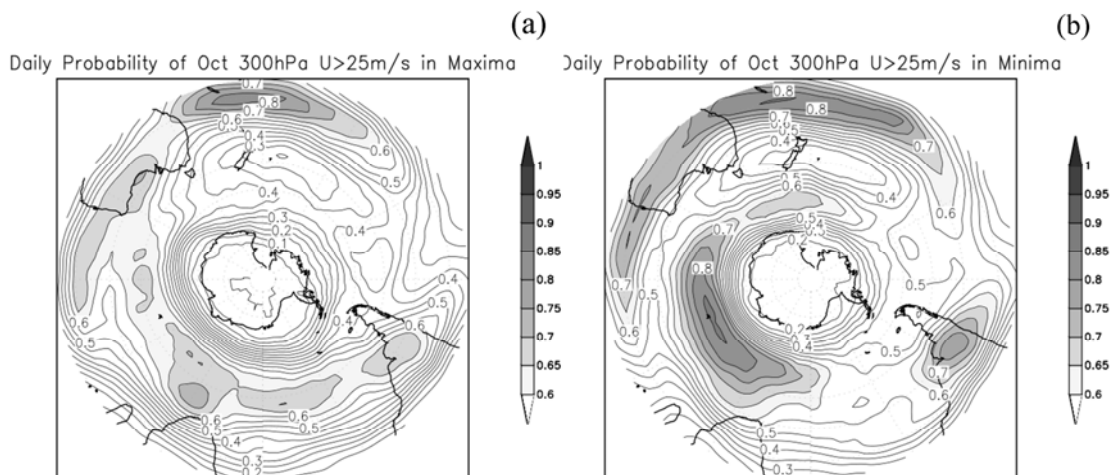


**Figure 8.** Daily Probability of zonal winds (U) over 25m/s at 300 hPa during Var Max maxima (a) and Max Var minima (b). Probabilities over 0.6 are shaded in grey scale.

A spiraling area of probability  $p > 0.65$  appears extending from subtropical South America towards the South Atlantic and midlatitude Indian Ocean. Hence over the Indian Ocean sector the probability of having a daily double jet occurrence (one at mid-to-subpolar latitudes and another at subtropical latitudes) is lower than 50%. The best case for double jet occurrence is to have one in the subtropical Pacific branch of the climatological jet ( $p \approx 0.80$ ) and another one south of South Africa over the Indian Ocean ( $p \approx 0.70$ ) which yields a joint probability of occurrence near 56%, which means close to 17 days in a month. On the other hand, during Var Max minima (when the midlatitude ozone trough is shifted to the east) the probability map distinctly yields daily double jet occurrence. Two main regions of peaking probabilities appear, one at low latitudes extending from the Indian towards the central Pacific Ocean ( $p > 0.80$ ), another at mid-to-subpolar latitudes over the Indian Ocean ( $p \approx 0.80$ ) that extends toward the Pacific Ocean south of New Zealand ( $p > 0.65$ ). A secondary area of high probabilities appears over subtropical South America ( $p > 0.70$ ). The best case for daily double jet occurrence is to have one in the broad subtropical Pacific Ocean sector ( $p \approx 0.85$ ) and another in the extended midlatitude Indian Ocean sector ( $p \approx 0.85$ ) yielding a probability of 72%, which means close to 22 days a month over any sector within those large probability areas.

Hence, the comparison between both probability fields shows enough evidence to conclude that during Var Max minima, i.e. when the midlatitude ozone negative lobe is eastward rotated, there is higher frequency of daily jets in the troposphere. In particular the polar jet is clearly active at daily scales at about  $30^{\circ}\text{E}$ - $90^{\circ}\text{E}$  and  $50^{\circ}\text{S}$  over the Indian Ocean just slightly westward and equatorward of the main tropospheric source of stratospheric stationary waves (compare with Fig. 6a-3). Bearing in mind that the divergence of the Plumb's stationary wave flux is not providing the exact location of the sources, but those can nevertheless be located somewhat upstream along the mean flow (Plumb 1985, 1989), then the synoptic eddy activity could be locally providing the wave energy for stationary waves according to the localized wave-propagation theory recently proposed by Nathan and Hodyss (2010). It can be said the same for a similar mechanism for the secondary maximum of subpolar daily tropospheric jets activity south of New Zealand and the stationary-wave source located over southern South Pacific.

## CONCLUSIONS

The present study has developed an index based on the maximum variance areas for residual TOC over the SH (Var Max) that is obtained after the removal of the contribution of important processes to TOC from its monthly mean observed fields, such as the 11-year solar cycle, the Brewer-Dobson meridional mass circulation and QBO. Such filtering thus allows the analysis of the dynamically induced TOC variability. Var Max index is used to study the interannual phase variability of the mid-to-high latitudes TOC trough as observed around and outside the polar vortex over southern South America and South Atlantic during October. Inspection of the residual TOC fields using the upper and lower quartiles of Var Max index distribution led to the classification of two extreme situations. The extreme maximum index values correspond to mid-to-high latitudes TOC minima (ozone trough) in the vicinity of southern South America, and the extreme minima index values to mid-to-high latitudes TOC minima (ozone trough) near the Greenwich Meridian. These situations reflect reasonably well the interannual longitudinal (phase) variation of the horseshoe-like spatial pattern of the mid-to-high latitudes TOC. Furthermore as extreme Var Max minima (negative midlatitude ozone lobe eastward rotated) are more frequent after the 1990s; the dynamical situation described for minima composites could suggest the existence of dynamic lower frequency processes associated with the eastward migration of the mean ozone trough position, observed in various studies, after the early 1990s.

It is found that both situations in residual TOC occur in response to significant temporal changes in the phase of the stratospheric geopotential height QSW1 due to an almost  $180^{\circ}$ -opposing anomalies located at high latitudes over South Pacific and the Indian Oceans (Fig. 5c and 5d). According to Moustouli *et al* (2003) the QSW1 perturbs the isentropic surfaces redistributing ozone so that the ozone field closely mimics the observed pattern in the stratospheric HGT field, and where the potential vorticity is weaker, non-reversible mixing of ozone-poor polar vortex air into southern midlatitudes is produced due to a wave breaking. Thus our results statistically support that the prevalent weaker meridional gradient along polar vortex edge and midlatitude trough sectors, are indeed acting as the dynamical containment vessel for minimum TOC residuals. We further show the manner in which the

residual TOC anomalies are associated with temporal anomalies perturbing the QSW1 phase whose origin appear to be mainly the troposphere.

When the ozone trough is in the vicinity of southern South America (Var Max index maxima composite), the QSW1 eddy is significantly intensified and located almost in the same position as the climatology eddy field is. The negative eddy lobe is accompanied by an active stationary-wave source region over the South Atlantic sector, where the upper troposphere and lower stratosphere seem to be coupled probably due to planetary waves generated by the interaction of mean flow and the orography of the southern tip of South America and the Antarctic Peninsula. During this state the probability of daily tropospheric jets is low in that area. Likewise the troposphere shows equatorward stormtracks migration and the stratospheric polar vortex intensity is significantly uncoupled with the lower stratosphere polar vortex intensity.

When the ozone trough is near the Greenwich Meridian (the Var Max index minima composite), the QSW1 eddy is significantly eastward shifted. This eastward rotation is accompanied by enhanced wave-stationary sources and sinks in the same regions as those of the climatology. The stationary-wave source regions over the Indian and southern Pacific Oceans are located somewhat poleward and eastward of the daily troposphere jets activity at mid-to-subpolar latitudes, possibly locally providing wave energy for the stratospheric wave anomalies (Nathan and Hodyss 2010). In this situation, the troposphere shows a “double” jet structure supported by higher daily double jets occurrence, some at subtropical-to-lower latitudes and others at mid-to-subpolar latitudes. The stratospheric polar vortex intensity resembles a solid body from lower to mid stratosphere. This extreme eastward rotation is more frequently observed after 1990; therefore, it is associated with the eastward migration of the mean midlatitude ozone trough position.

In agreement with Huth and Canziani (2003) that observed changes in the stratosphere, Barrucand *et al.* (2008) suggest that during early 1990s there is a change in the SH annular mode (SAM) interannual variability towards higher frequencies during spring, which means changes in the vacillation state of zonal winds maximum and middle and higher latitudes. Furthermore Udagawa *et al* (2009) noted that the eastward migrations in Antarctic Sea Ice Content, which occurred between 1984 and 1994, could be linked to changes in tropospheric circulation, associated with modifications in the relative contributions of SAM and PSA (Pacific South Atlantic) modes. These authors argue that their results support the presence of atmospheric climate shifts. Hence the eastward migration of the midlatitude ozone trough between the 80s and 90s could be linked to the changes in the SAM interannual variability and the way that troposphere and stratosphere couple. Further analysis is needed to understand the nature of these atmospheric changes as well as the role played by the synoptic wave activity in the troposphere/stratosphere coupling at interannual scales during austral spring.

### **Acknowledgments**

The authors wish to thank the funds received from CONICET (PIP 2004 5276), PICT 2007 ICES-IDAC 01888, ANPCyT PICT-2007-00438 and UCA (PEPACG) which made this research possible. Also thanks to Carmelite Order.

### **REFERENCES**

- Barrucand, M., M. Rusticucci, and W. Vargas, 2008. Temperature extremes in the south of South America in relation to Atlantic Ocean surface temperature and Southern Hemisphere circulation. *J. Geophys. Res.*, 113, D20111, doi:10.1029/2007JD009026.
- Bischoff, S.A. P.O. Canziani, A.E. Yuchechen, 2007. The tropopause at southern extratropical latitudes: Argentine operational rawinsonde climatology, *Int. J. Climat.*, 27: 189–209 DOI: 10.1002/joc.1385
- Canziani, P.O. W. E. Legnani 2003. Tropospheric-Stratospheric Coupling: Extratropical synoptic systems in the lower stratosphere, *Quart. J. Roy Meteorol. Soc.*, 129
- Canziani, P.O., F.E. Malanca, E.A. Agosta, 2008. Ozone and UT/LS variability and change at Southern midlatitudes: 1980-2000: decadal variations. *J. Geophys. Res.*, 113, D20101, doi:10.1029/2007JD009303.
- Grytsai, A., Z. Grytsai, A. Evtushevsky, G. Milinevsky, and N. Leonov, 2005. Zonal wave numbers 1–5 in planetary waves from the TOMS total ozone at 65° S, *Ann. Geophys.*, 23, 1565–1573

- Grytsai A. V., Evtushevsky O. M., Agapitov O. V., Klekociuk A. R., and G. P. Milinevsky 2007. Structure and long-term change in the zonal asymmetry in Antarctic total ozone during spring, *Ann. Geophys.*, 25, 361–374.
- Hio, Y., and I. Hirota, 2002. Interannual Variations of Planetary Waves in the Southern Hemisphere Stratosphere, *J. Met. Soc. Jpn.*, 80, 1013-1027.
- Huth, R. , Canziani, P.O., 2003. Classification of hemispheric monthly mean stratospheric potential vorticity fields, *Annales Geophysicae*, 21, 805-817.
- Inatsu M, Hoskins BJ, 2004. The Zonal Asymmetry of the Southern Hemisphere Winter Storm Track. *J. Climate*, 17, 4882- –4892.
- Karoly D.J., Plumb R.A. and Ting M., 1989. Examples of the Horizontal Propagation of Quasi-stationary Waves. *J. Atmos. Sci.*, 46, 2802–2811. DOI: 10.1175/1520-0469.
- Labitzke J.G. and H. Van Loon, 1999. *The Stratosphere. Phenomena, History and Relvance*. Springer-Verlag, Berlin, 180p
- Malanca, F.E., P. O. Canziani, G. Argüello, 2003. Total ozone variability and change at southern mid-latitudes, *Revista Meteorológica (Argentina)*, , 28, 53-62.
- Malanca, F.E., P.O. Canziani, G.Argüello, 2005. Trends evolution of ozone between 1980 and 2000 at mid-latitudes over the Southern Hemisphere. Decadal differences in trends, *J. Geophys. Res.* 110, D05102, doi:10.1029/2004JD004977
- Moser, B.K., G.R., Stevens , and C.L., Watts, 1989. The two-sample t-test versus Satterwaite’s approximate F test, *Commun. Stat. Theory Methodol.*, 18, 3963-3975.
- Moser, B.K., G.R. Stevens, 1992. Homogeneity of variance in the two-sample means test, *Am. Stat.*, 46, 19-21
- Moustaoui, M., H. Teitelbaum, and F. P. J. Valero, 2003. Vertical displacements induced by quasi-stationary waves in the Southern Hemisphere stratosphere during spring, *Q. J. R. Meteorol. Soc.*, 131,2279– 2289
- Nathan T. and D. Hodyss, 2010. Troposphere-stratosphere communication through local vertical waveguides. *Q.J.R. Meteorol. Soc.* 136:12-19.
- Rao, V. Brahmananda, J. P. R. Fernandez, and S. H. Franchito, 2004. Quasi-stationary waves in the Southern Hemisphere during El Niño and La Niña events. *Annales Geophysicae*, 22, 789–806.
- Pan LL, Randel WJ, Gary BL, Mahoney MJ, Hintsaj EJ, 2004. Definitions and sharpness of the extratropical tropopause: a trace gas perspective. *J. Geophys. Res.*, 109-125.
- Plumb, R.A., 1985. Onthree-Dimension Propagation of Stationary Waves, *J. Atmos. Sci.*, 42, 217-229.
- Plumb, R.A., 1989. On The Seasonal Cycle of Stratospheric Planetary Waves, *PAGEOPH*, 130, 233-242.
- Trenberth, K.E., 1991. Storm tracks in the southern hemisphere. *J. Atmos. Sci.*, 48, 2159-2178.
- Udagawa, Y., Y. Tachibana, and K. Yamazaki, 2009. Modulation in interannual sea ice patterns in the Southern Ocean in association with large-scale atmospheric mode shift, *J. Geophys. Res.*, 114, D21103, doi:10.1029/2009JD011807
- Ziemke, J.R., Chandra, S., R.D. Mc Peters, P.A. Newman, 1997. Dynamical proxies of total ozone with applications to global trend models, *J. Geophys. Res.*, 10, 6117-6129.